Research Article
Volume 13:5, 2023

Medicinal Chemistry

ISSN: : 2161-0444 **Open Access**

Molecular Docking, Synthesis and Preliminary Evaluation of Hybrid Molecules of Benzothiazole Cross-linked with Hydroxamic Acid by Certain Linkers as HDAC Inhibitors

Yazen Abdul-Hameed[1], Shakir M. Alwan[2*] and Ashour H. Dawood[3]

[1]Department of Pharmaceutical Chemistry, College of Pharmacy, Al-Mustanseryia University, Baghdad, Iraq

[2]Department of Pharmacy, Al-Farabi University College, Baghdad, Iraq

[3]Department of Pharmaceutical Chemistry, Al-Esraa University, Baghdad, Iraq

Abstract

Molecular hybridization in drug design is proved to be very successful approach to provide new chemical entities with potential activities and desirable physicochemical properties. Histone Deacetylases (HDACs) are a group of enzymes that are involved in controlling the behavior and route of acetylation of histone and non-histone proteins. Inhibition of HDACs causes inhibition of cell growth, differentiation, changes in gene expression and death. Hybrid molecules of Benzothiazole cross-linked with hydroxamic acid through an amino acid or aminoalkanoic acid were considered. The suggested hybrids (2A-E) were subjected to molecular docking to evaluate their binding affinities with HDAC8 (PDB ID: 1T69). These hybrids (2A-E) recorded lower △G (-8.117, -6.322, -8.16, -7.939, - 9.46, respectively) than Vorinostat (suberoylanilide hydroxamic acid, SAHA), as the reference ligand (-5.375). Compound 2E (Benzothiazole cross-linked with hydroxamic acid by a p-aminobenzoic acid) has recorded the lowest docking score of -9.460 and this may indicate that it has the highest inhibitory activity. Docking scores represent the required energy for binding to receptor and calculated as △G (kcal/mol). Computational methods for the characterization of the investigated hybrids were employed using the SwissADME server to predict the ADME parameters (Absorption, Distribution, Metabolism and Excretion) and other physicochemical properties. Hybrids showed no violations from Lipinski's rule and complied with all parameters. As indicated from the predicted results, all hybrids have low possible passive oral absorption and no penetration into BBB. The hybrids 2B and 2D may be considered as P-gp substrates. SAHA does not inhibit any of the CYP enzymes used in this study, while, the hybrids 2B, 2D and 2E have shown possible inhibitory activities. These interesting results are very encouraging to proceed for the synthesis of these successful candidates and performing cytotocity evaluation. The hybrids 2D and 2E showed significant and remarkable activity on lung cancer cell line type A549, in comparison with SAHA results.

Keywords: Hydroxamic acid • Molecular hybridization • Benzothiazole • HDACs inhibitors

Introduction

Benzothiazole (BZT) is a fused ring of benzene and thiazole and has been intensively studied, as one of the privileged pharmacophores in medicinal chemistry [1]. BZT has emerged as a core structure for diversified therapeutic applications, such as, antioxidant, anticancer, antiviral anti-proliferative, anti-diabetic, analgesic, anti-malarial, anti-fungal, anti-histamine and anti-convulsant [2]. BZT scaffolds showed a crucial role in the inhibition of the tumor-associated metalloenzyme carbonic anhydrase and consequently, serve as anticancer agents [3]. Research has revealed that inhibition of histone deacetylases (HDACs) causes inhibition of cell growth, differentiation, changes in gene expression and death [4,5]. HDACs inhibitors have relatively low toxicity toward normal cells, while, inhibiting tumor cells from proliferation and survival. The first FDA-Approved HDACs inhibitor was the hydroxamate, Vorinostat (suberoyl-anilide hydroxamic acid, SAHA), which is used for treating cutaneous T-cell lymphoma [6]. When HDACs activity is inhibited, the balance between the conflicting activities of HATs (histone acetylates) and HDACs shifts towards the predominance of HAT activity, leading to the induction of acetylation of both histone and non-histone proteins. As a result, certain genes that influence gene expression will be influenced by the induction or silencing of transcription factor expression as well as certain proliferative and/or apoptotic genes [7]. As a result, HDACIs may activate pathways that lead to apoptosis DNA replication is hindered, the cell cycle is stopped, proliferation is stimulated, angiogenesis is decreased, DNA fragmentation is promoted, and the angiogenesis is minimized. All of which can result in the death of cancer cells [8,9]. The development of hybrid multifunctional inhibitors has generated a lot of interest in the search for new medicines. Hybrid molecules have the potential to simultaneously act on two or more cancer-relevant targets, such as, metallo-proteinase. ATP binding cassette subfamily G member 2, human mitochondrial peptide deformylase, nuclear factor kappa light-chain-enhancer of activated B cells, P-glycoprotein, tubulin and vascular endothelial growth factor [10-12]. Various hybrid molecules of hydroxamic acid have antiproliferative and anticancer activities and certain hybrids possess great potency against both drug-sensitive and drug-resistant cancers [13]. 2-Aminobenzothiazole derivatives containing hydroxamic acid were reported to have potent histone deacetylase inhibitory and antitumor activities [14]. Hydroxamic acid derivatives prepared by the reaction of 2-aminobenzo-thiazole with adipic acid have exhibited good anticancer activities against five different cell lines such MCF-7, AsPC-1, SW620, PC3 and NCI-H460 [15]. Due to their reduced risk of adverse drug-

***Address for Correspondence:** Shakir M. Alwan, Department of Pharmacy, Al-Farabi University College, Baghdad, Iraq, E-mail: shakir.alwan@alfarabiuc.edu.iq*

Received: 20 September, 2023, Manuscript No. mccr-23-114376; **Editor Assigned:** 22 September, 2023, PreQC No. P-114376; **Reviewed:** 03 October, 2023, QC No. Q-114376; **Revised:** 09 October, 2023, Manuscript No. R-114376; **Published:** 16 October, 2023, DOI: 10.37421/2161-0444.2023.13.687

drug interactions than multicomponent medications, hybrid molecules can also counteract the recognized side effects associated with various hybrid elements. As a result, one of the most popular contemporary methods for preparing new anticancer drugs is hybridization [16].

In view of the previous findings, a new approach of preparing hybrid molecules of BZT cross-linked with hydroxamic acid *via* L-Alanine, L-Cysteine, 3-Aminopropionic acid, 6-Aminohexanoic acid and p-Aminobenzoic acid, as the linkers, was considered. This approach may lead to the optimization of the pharmacological activities of the proposed compounds, especially the antitumor activity.

Materials and Methods

Chemicals: 2-Mercaptobenzothiazole, p-amino- benzoic acid, 3-aminopropionic acid, 6-aminohexanoic acid was purchased from Hyperchem/China. Ethyl Chloroformate (ECF), Hydroxylamine. HCl and the amino acids were supplied by Sigma Aldrich /Germany. Vorinostat (suberoylanilide hydroxamic acid, SAHA), L-Alanine, L-Cysteine, aminopropionic acid, aminohexanoic acid and p-aminobenzoic acid were purchased from sigma/Aldrich (Germany). For cell culture studies all the investigated compounds were dissolved in Dimethyl sulfoxide (DMSO, 10 mM stocks) and stocks stored at -20 °C. For the experiments, stocks were diluted in cell culture medium (DMSO concentrations were always <1%. The hybrid molecules were synthesized as described in details in the following section.

Preparation of the investigated hybrid molecules: Hybrid molecules of Benzothiazole cross-linked with hydroxamic acid through certain linkers, such as, L-alanine, L-cysteine, amino propionic acid, amino hexanoic acid or p-amino-benzoic acid were proposed. These hybrid molecules were prepared starting from 2-mercaptobenzo-thiazole, which is S-alkylated with bromoacetic acid leading to the formation of Benzothiazole containing a side chain with a sulfide and a carboxyl group, as called the intermediate (2-(benzo[d]thiazol-2-yl-thio) acetic acid). The chemical structures of the new hybrids (Figure 1) and their SMILES (Simplified Molecular-Input Line-Entry Systems) notations were constructed using Chemdraw ultra 10.0. Vorinostat (suberoylanilide hydroxamic acid, SAHA) was used as the reference ligand.

Molecular docking: Molecular docking was performed using the Maestro software (Schrödinger, version 2023-1) and the △G (kcal/mol) values, as the docking scores function representing the energy required for binding to receptor, were calculated. The chemical structure of HDAC8 type 1T69 was retrieved from protein data bank, PDB, website (https://www.rcsb.org) and imported to Maestro software program. They were processed and their energy was minimized by the Protein Preparation Workflow module. Through this process, unnecessary metals (except Zn+2 ions), ligands (except SAHA, which is the reference ligand), enzyme chains (except chain A), and the water molecules were deleted. The Grid was generated by the Receptor Grid Generator module, during which the binding site was defined by SAHA. The lowest docking scores, as △G (kcal/mol), for the investigated compounds and their images, which showed the interaction of each compound with Zn2+ ions and the amino acid residues in the binding site. Docking scores and visualization images of ligand-receptor complexes were shown on Table 1-3 and Figure 2. These hybrids were treated as successful candidates that have the highest binding affinities based on the lowest docking scores (ΔG, Kcal/mole).

General methods: Melting points were determined (uncorrected) using electrical melting point apparatus, Electro-thermal 9300, USA. The infrared

Table 1. Docking scores of SAHA and the target compounds 2A-E, and their interaction with the amino acid residues in or near the active site of HDAC8 (PDB ID:1T69).

Compound	Docking Scores of the Investigated Compounds with HDAC8 type 1T69 ΔG (kcal/mol)	Amino acid Residues of HDAC8 type 1T69 Involved in the Interaction
SAHA	-5.357	Asp101, His142, Tyr306, Zinc378
2A	-8.117	His142, Phe207, Tyr306, Zinc378
2B	-6.322	His142, Tyr306, Zinc378
2C	-8.16	His142, Phe207, Tyr306, Zinc378
2D	-7.939	His142, His180, Lys202, Phe207, Tyr306, Zinc378
2E	-9.46	His142, Tyr306, Zinc 378

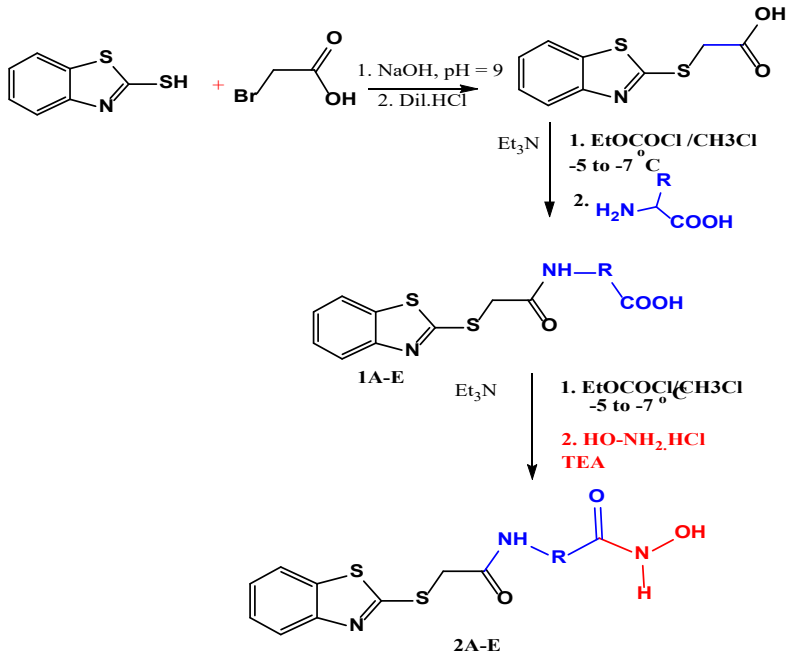

Figure 1. Chemical synthesis of the hybrid molecules of benzothiazole-hydroxamic acid cross-linked by certain linkers.

spectra were recorded in KBr disc by FT-IR spectrophoto- meter / Shimadzu. 1H-NMR and 13C-NMR spectra were recorded using NMR Bruker 500 MHz–Avance III spectrometer and the chemical shifts were recorded in Parts Per Million (ppm). Tetramethylsilane was used as the reference.

Chemical synthesis

Chemical synthesis of the intermediate (2-(benzo[d]thiazol-2-yl-thio) acetic acid: This compound is prepared through S-alkylation reaction of 2-mercaptobenzothiazole with α-bromoacetic acid, and as follows;

To a stirred aqueous solution of -bromoacetic acid (10 mmol, 1.389 g) in sodium hydroxide solution (10%, 10 ml), 2-mercaptobenzothiazole (10 mmol, 1.6725 g) in 10% aqueous solution of sodium hydroxide (10 ml) was added . The mixture was refluxed for 3 hrs and was then cooled and acidified with diluted hydrochloric acid to obtain a precipitate, which was filtered, washed excessively with distilled water and crystallized from ethanol to afford a yield of 90%, as white powder, m.p. 152-153 °C, as depicted on Figure 1.

FT-IR spectra recorded the following bands; 3110-2513 (str. vib. of OH of COOH), 3074 (Str. vib. of C-H aromatic ring), 2956-2896 (str. vib. of C-H aliph. (asym and sym), 1714 (str. vib. of C=O of COOH), 1602-1581-1498 (str. vib. of C=C aromatic ring), 1315 (Str. vib. of C-O of COOH).

General procedure for the synthesis of BZT-Linker (1A-E): These compounds were prepared using the mixed anhydride method 17, as depicted in Figure 1 and as follows;

The intermediate (2-(benzo[d]thiazol-2-yl-thio) acetic acid (10mmol) was suspended in dry chloroform (40ml) containing triethylamine (TEA, 10 mmol) and the mixture was cooled to (-5 to -8 °C) in an ice bath. Ethyl chloroformate (10 mmol) was added dropwise during 15 min and the mixture was stirred for further 15 min. The amino acid or the linker (10 mmol) was dissolved in a cold distilled water containing TEA (10mmol) and was added immediately all at once with vigorous stirring for 1hr in an ice bath and for further 3hrs at room temperature. A two-layered yellowish-orange solution was obtained, which was separated using a separator funnel and the aqueous layer was removed. The aqueous layer was acidified with a few drops of hydrochloric acid (1N) to adjust the pH to 3-4. A small amount of a precipitate was formed, which is the unreacted intermediate and was removed by filtration. The chloroform layer was washed with distilled water (3 × 20 ml) and was dried with anhydrous magnesium sulfate and filtered, evaporated under reduced pressure in a rotary evaporator to obtain yellowish-orange residues. The residues were washed with diethyl ether or petroleum ether few times to afford crystalline powder representing the resultant products (1A-E). The following compounds were synthesized; Compound 1A {(2-(benzo[d]thiazol-2-yl-thio) acetyl) alanine ($C_{12}H_{12}O_3N_2S_2$, 296.36 g/mole)} was synthesized starting from the intermediate (2-(benzo[d]thiazol-2-yl-thio) acetic acid) and L-Alanine (10mmol, 1.6g), as red crystalline powder, 165-167 °C with 79% yield. FT-IR spectra (cm-1, υ) recorded the following characterized bands; 3461 (str. vib. of OH-COOH), 3419 (str. vib. of NH-amide), 2954-2905 (str. vib. of C-H aliph. (asym and sym), 1712 (str. vib. of C=O of COOH), 1668 (str. vib. of C=O of amide), 1589-1573-1479 (str. vib. of C=C aromatic ring).

Compound 1B {(2-(benzo[d]thiazol-2-yl-thio) acetyl) cysteine ($C_{12}H_{12}O_3N_2S_3$, 328.42 g/mole)} was prepared using L-Cysteine (10 mmol, 1.2 g) and collected as yellow crystalline powder, 175-177 °C with 85% yield. FT-IR spectra recorded the following bands; 3461 (str. vib. of OH-COOH), 3288 (str. vib. of NH-amide), 3062 (str. vib. of C-H aromatic ring), 2912-2871 (str. vib. of C-H aliph. (asym and sym), 1714 (str. vib. of C=O of COOH), 1641 (str. vib. of C=O of amide), 1600-1545 (str. vib. of C=C aromatic ring).

Compound 1C {3-(2-(benzo[d]thiazol-2-yl- thio) acetamido) propionic acid ($C_{12}H_{12}O_3N_2S_2$, 296.36) was prepared by reacting the intermediate with 3-Aminopropionic acid (10 mmol,1.6 g) and collected as orange powder, 210-212 °C with 76% yield. FT-IR spectra recorded the following bands; 3442(str. vib. of OH-COOH), 3225 (str. vib. of NH amide), 3050 (str. vib. of C-H aromatic ring), 2987-2858 (str. vib. of C-H aliph. (asym and sym), 1724 (str. vib. of C=O of COOH), 1631 (str. vib. of C=O of amide), 1600-1514 (Str. vib. of C=C aromatic ring).

Compound 1D {6-(2-(benzo[d]thiazol-2-yl-thio) acetamido) hexanoic acid ($C_{15}H_{18}O_3N_2S_2$, 338 g/mole)} was prepared starting from the intermediate and 6-Aminohexanoic acid (10mmol, 1.31g) and collected as orange powder, 225-227 °C with 90% yield. FT-IR spectra recorded the following bands; 3427 (str. vib. of OH-COOH), 3271(str. vib. of NH of amide), 3075 (str. vib. of C-H arom), 2983-2873 (str. vib. of C-H aliph. (asym and sym), 1737 (str. vib. of C=O of COOH),1629 (Str. vib. of C=O of amid),1612-1581 (str. vib. of C=C arom).

Compound 1E {4-(2-(benzo[d]thiazol-2-yl-thio) acetamido) benzoic acid ($C_{16}H_{12}O_3N_2S_2$, 344.4 g/mole)} was prepared from the intermediate and p-Amino-benzoic acid (10 mmol, 1.37 g) and collected as purple powder, 180-182 °C with 70% yield. FT-IR spectra recorded the following bands; 3430 (str. vib. of OH-COOH), 3330 (str. vib. of NH of amide), 3026 (str. vib. of C-H arom), 2981-2937 (str. vib. of C-H arom), 1703 (str. vib. of C=O of COOH), 1641(str. vib. of C=O of amide), 1598-1558-1479 (str. vib. of C=C arom).

General procedure for preparing compounds 2A-E: The target hybrid molecules were prepared starting with compounds 1A-E and reacted with hydroxylamine to afford compounds 2A-E, as depicted in Figure 1. This reaction was performed using the mixed anhydride method [17], as previously described. Compounds 1A-E (10 mmol) in dry chloroform containing TEA (10 mmol) was reacted with ECF (10 mmol) and was then reacted with hydroxylamine. HCl (10 mmol) in an aqueous solution (10 ml) containing TEA (10 mmol).

The hybrid 2A {2-(2-(benzo- [d]thiazol-2-yl-thio) acetamido)-N-hydroxypropan- amide: ($C_{12}H_{13}O3N3S2$, 311.37 g/mole) was prepared using compound 1A (10mmol, 2.964 g) and was collected as yellow powder, 253-255 °C with 80% yield. FT-IR spectra recorded the following bands;

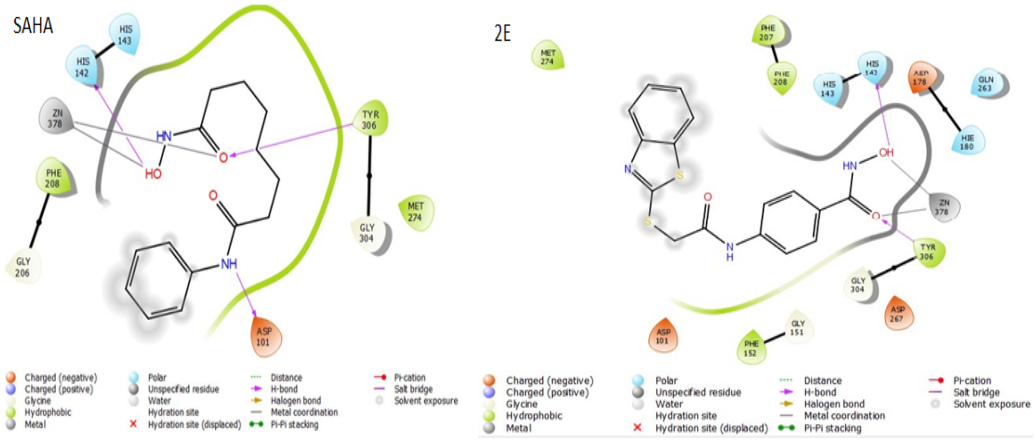

Figure 2. Interaction of SAHA and compound 2E with the amino acid residues at the catalytic pocket of HDAC8 (PDB ID: 1T69).

3452 (OH str. vib. of oxime), 3257 (NH str. vib. of oxime), 3200 (NH str. vib. of amide), 3058 (str. vib. of C-H arom), 2983-2852 (str. vib. of C-H aliph. (asym and sym), 1699 (str. vib. of C=O of oxime),1616 (str. vib. of C=O of amide), 1610-1569 (str. vib. of C=C arom). 1H-NMR spectra recorded the followings signals (ppm); 1.28 (doublet, 3H), (CH_3), 4.25 (quartet,1H, CH), 4.92(singlet, 2H, CH_2), 7.40- 8.35 (multiplate, 4H) represent phenyl), 8.85 (singlet 1H, NH of amide group), 9.20 (singlet 1H, NH of oxime group), 10.96 (singlet, 1H, OH group). 13C-NMR spectra recorded the followings signals; 13.67 (CH_3), 34.59 (CH), 61.50 (CH_2), 111.91 (arom. CH), 120.32 (arom CH), 121.38 (arom CH), 123.96 (arom CH), 124.21 (arom CH), 125.83 (arom CH), 152.58 (C=N of Benzothiazole), 164.54 (C=O of amide), 168.09 (C=O of oxime).

The hybrid 2B{2-(2-(benzo[d]thiazol-2-yl-thio) acetamido)-N-hydroxy-3-mercapto propanamide ($C_{12}H_{13}O_3N_3S_3$, 343.43 g/mole) was prepared starting from compound 1B (10mmol, 3.284 g) and was collected as paige-colored powder, 235-237 °C with 77% yield. FT-IR spectra recorded the followings; 3431 (OH str. vib. of oxime), 3290 (NH str. vib. of oxime), 3114 (NH str. vib. of amide), 3078 (str. vib. of C-H aromatic ring), 2964-2894 (str. vib. of C-H aliph. (asym and sym), 1699 (str. vib. of C=O of oxime), 1639 (str. vib. of C=O of amide), 1596-1554-1496 (str. vib. of C=C arom.).

1H-NMR spectra recorded the followings; 3.50 (doublet, 2H, CH_2), 4.19 (triplet, 1H, CH), 4.5 (singlet, 2H, CH_2), 4.88 (singlet, 1H, SH), 7.40-8.35 (multiplate, 4H, phenyl), 8.85 singlet, 1H, NH of amide group, 9.20 singlet, 1H, NH of oxime group, 10.96 (singlet, 1H, OH group).

13C-NMR spectra recorded the followings; 39.66 (CH_2-SH), 40.78 (CH), 41.23 (CH_2), 124,86 (CH arom), 126.85 (CH. arom),127.83 (CH. arom), 128.06 (CH, arom) 133.68 (CH- arom),135.25 (CH. arom),153.32 (C=N of Benzothiazole), 158.61 (C=O of amide), 167.27 (C=O of oxime).

The hybrid 2C {3-(2-(benzo[d]thiazol-2-yl-thio) acetamido)-N-hydroxypropanamide: ($C_{12}H_{13}O_3N_3S_2$, 311.37 g/mole)} was prepared starting from compound 1C (10mmol, 2.964 g) and was collected as dark brown powder, 219-221 °C with 88% yield. FT-IR spectra recorded the following bands; 3315 (OH str. vib. of oxime), 3188 (NH str. vib. of oxime), 3112 (NH str. vib. of amide), 3053 (str. vib. of C-H arom.), 2981-2837 (str. vib. of C-H aliph. (asym and sym), 1704 (str. vib. of C=O of oxime), 1679 (str. vib. of C=O of amide), 1600-1531-1500 (str. vib. of C=C arom.). 1H-NMR spectra recorded the followings; 2.16(triplet, 2H, CH_2-C=O), 3.58 (triplet, 2H, CH_2-N), 4.32(singlet, 2H, CH_2-S), 7.32-8.20 (multiplate, 4H, phenyl, 8.90 (singlet, 1H, NH of amide), 8.94 (singlet, 1H, NH of oxime), 9.86 (singlet, 1H, OH).

13C-NMR spectra recorded the followings; 19.05 (CH_2-C=O), 38.30 (CH_2-N), 56.53 (CH_2-S), 119.31 (CH arom), 124.84 (CH arom), 125.06 (CH arom), 126.91 (CH arom), 129.06 (CH arom), 129.34 (CH arom), 152.97 (C=N of Benzothiazole), 166.37 (C=O of amide), 166.59 (C=O of oxime).

The hybrid 2D {6-(2-(benzo[d]thiazol-2-yl-thio) acetamido)-N-hydroxyhexanamide: ($C_{15}H_{19}O_3N_3S_2$, 353.45 g/mol) was synthesized from compound 1D (10mmol, 3.38 g) and was collected as chocolate-color powder, 269-271 °C with 85% yield. FT-IR spectra recorded the following bands; 34446 (str. vib. of OH-oxime), 3359 (str. vib. of NH-oxime), 3184 (NH str. vib. of amide), 3060 (str. vib. of C-H arom.), 2985-2918 (str. vib. of C-H aliph. (asym and sym), 1704 (str. vib. of C=O of oxime), 1649 (str. vib. of C=O of amide), 1599-1583(str. vib. of C=C arom.). 1H-NMR spectra recorded the followings; 1.25-2.11(Multiplate, 6H, 3(CH_2), 4.14 (triplet, 2H, CH_2-C=O), 4.19 (triplet, 2H, CH_2-N), 4.87 (singlet, 2H, CH_2-S),7.35-8.05 (multiplate, 4H, phenyl), 8.32(singlet, 1H, NH of amide), 8.86 (singlet, 1H, NH of oxime), 10.20 (singlet, 1H, OH). 13C-NMR spectra recorded the followings; 13.78 (CH_2), 18.25 (CH_2), 20.89 (CH_2), 24.60 (CH_2 C=O), 35.86 (CH2 -N), 55.86 (CH_2-S), 111.86-134.90(CH arom), 151.03 (C=N of Benzthiazole), 158.84 (C=O of amide), 162.32 (C=O of oxime).

The hybrid 2E {4-(2-(benzo[d]thiazol-2-yl-thio) acetamido)-N-Hydroxy benzamide: ($C_{16}H_{13}O_3N_3S_2$, 359.42 g/mole) was prepared starting from compound 1E (10 mmol, 3.44 g) and was collected as white powder, 280-282 °C with 90% yield. FT-IR spectra recorded the following bands; 3444(OH str. vib. of oxime), 3404 (NH str. vib. of oxime), 3295 (NH str. vib. of oxime), 3022 (str. vib. of C-H arom), 2972-2925 (str. vib. of C-H aliph. (asym and sym), 1685 (Str. vib. of C=O of oxime), 1625 (str. vib. of C=O of amide), 1597-1546 (str. vib. of C=C arom). 1H-NMR spectra recorded the followings; 4.12 (singlet, 2H, CH_2-S), 7.28-7.30 (doublet, 2H, CH far C=O), 7.31-7.82 (multiplate, 4H, CH of Benzothiazole),7.91-7.94 (doublet, 2H, CH near C=O), 8.35 (singlet, 1H, NH of amide group),9.35 (singlet, 1H, NH of oxime), 10.78 (singlet, 1H, OH). 13C-NMR spectra recorded the followings; 41.12 (CH_2-S), 116.28 (CH arom), 121.58 (CH arom), 122.25 (CH, arom), 124.84 (CH arom), 126.83 (CH arom), 127.83 (CH arom), 128.08 (CH arom), 133.68 (CH arom), 135.21 (CH arom), 137.12 (CH arom), 153.61 (C=N of Benzothiazole), 158.62 (C=O of amide), 167.22 (C=O of oxime).

Cell culture

Detailed information as well as culture and MTT seeding conditions for used cell lines are provided. All cells were grown under standard cell

Table 2. Drug likeness parameters for SAHA and the target compounds 2A-E.

Compound	Drug Likeness				
	Lipinski	Ghose	Veber	Egan	Muegge
SAHA	Yes		Yes	Yes	Yes
2A	Yes	Yes	1 violation: TPSA >140	1 violation: TPSA >131.6	Yes
2B	Yes	Yes	1 violation: TPSA >140	1 violation: TPSA >131.6	1 violation: TPSA >150
2C	Yes	Yes	1 violation: TPSA >140	1 violation: TPSA >131.6	Yes
2D	Yes	Yes	2 violations: Rotors >10, TPSA >140	1 violation: TPSA >131.6	Yes
2E	Yes	Yes	1 violation: TPSA >140	1 violation: TPSA >131.6	Yes

Table 3. The pharmacokinetic properties of SAHA and the target compounds 2A-E.

Parameter	Compound					
	SAHA	2A	2B	2C	2D	2E
Passive GI absorption	High	Low	Low	Low	Low	Low
BBB permeability	Yes	No	No	No	No	No
P-gp substrate	No	No	Yes	No	Yes	No
CYP1A2 inhibitor	No	No	No	No	No	No
CYP2C19 inhibitor	No	No	Yes	No	No	Yes
CYP2C9 inhibitor	No	No	No	No	Yes	Yes
CYP2D6 inhibitor	No	No	No	No	No	Yes
CYP3A4 inhibitor	No	No	No	No	Yes	Yes
Log Kp (skin permeation) cm/s	-6.23	-6.79	-7.15	-7.31	-6.75	-6.43

culture conditions and regularly checked for mycoplasma contamination. The medium was supplemented with 10% fetal bovine calf serum.

Cell viability assays

Cells were plated (depending on the cell model 2-7 × 103 cells/well) in 96-well plates and allowed to recover for 24 h, 48 h and 72 h. Subsequently, the indicated drugs or their combinations were added. After 72 h exposure, the proportion of viable cells was determined by MTT assay [18]. Cytotoxicity was expressed as IC50 (μg/ml) values calculated from full dose-response curves using Graph Pad Prism 8 software. The new hybrid molecules (2A-E) were tested for their anticancer activities using a colorimetric assay on the A549 human lung cancer cell [18]. MTT stock solution was added and the mixture was stored to generate purple formazan crystals for 2-4 h at 37 °C. MTT solution was correctly disposed, formazan crystal was mixed in DMSO (100 μl) containing SDS (10%) and acetic acid (1%). To completely dissolve the formazan crystals, the plates were agitated on the top of a shaker for 10 min. The procedure was done in 96-well flat plates at different concentrations (500-0.97 μM) of the investigated compounds and the IC50 values were calculated after treating the cells with the compounds for 24, 48 and 72 hrs. Cell culture medium was carefully removed after being treated with the hybrids. The optical density was obtained at 570 nm and a Safire 2 Microplate reader were used to calculate the concentrations. The experiments were carried out in triplicate independently. The results are presented on Table 4. The dose-response curves were done by Prism Pad 9 using nonlinear regression analysis for the synthesized molecules using A549 cells are shown on Figure 3.

Results

Molecular docking

All the investigated compounds (2A-E) have shown very interesting results of interaction pattern with the amino acids of HDAC8 (PDB ID: 1T69). These compounds have recorded high binding affinities, as indicated from the low docking scores, expressed as △G (Kcal/mol) than SAHA (Table 1). Moreover, compound 2E (BZT linked to hydroxamic acid by p-aminobenzoic acid, recorded the lowest docking score -9.460). This may indicate that this compound has the highest HDAC8 inhibitory activity.

Prediction of physicochemical and ADME properties

The SwissADME server was employed for the prediction of the physicochemical and ADME properties of the investigated compounds in comparison with SAHA. The pharmacokinetic parameters of these target compounds have shown variation in properties according to chemical

Table 4. The IC50 values of compounds 2A-E and SAHA against lung cancer cell line (A549).

Compound	Half-maximum Inhibitory Concentration IC50 μg/ml		
	Incubation Time (hrs)		
	24	48	72
SAHA	145.7	64.26	31.16
2A	-	-	-
2B	139	45.45	24.95
2C	221	108.73	50.21
2D	149	80.48	17.3
2E	103.9	42.25	15.45

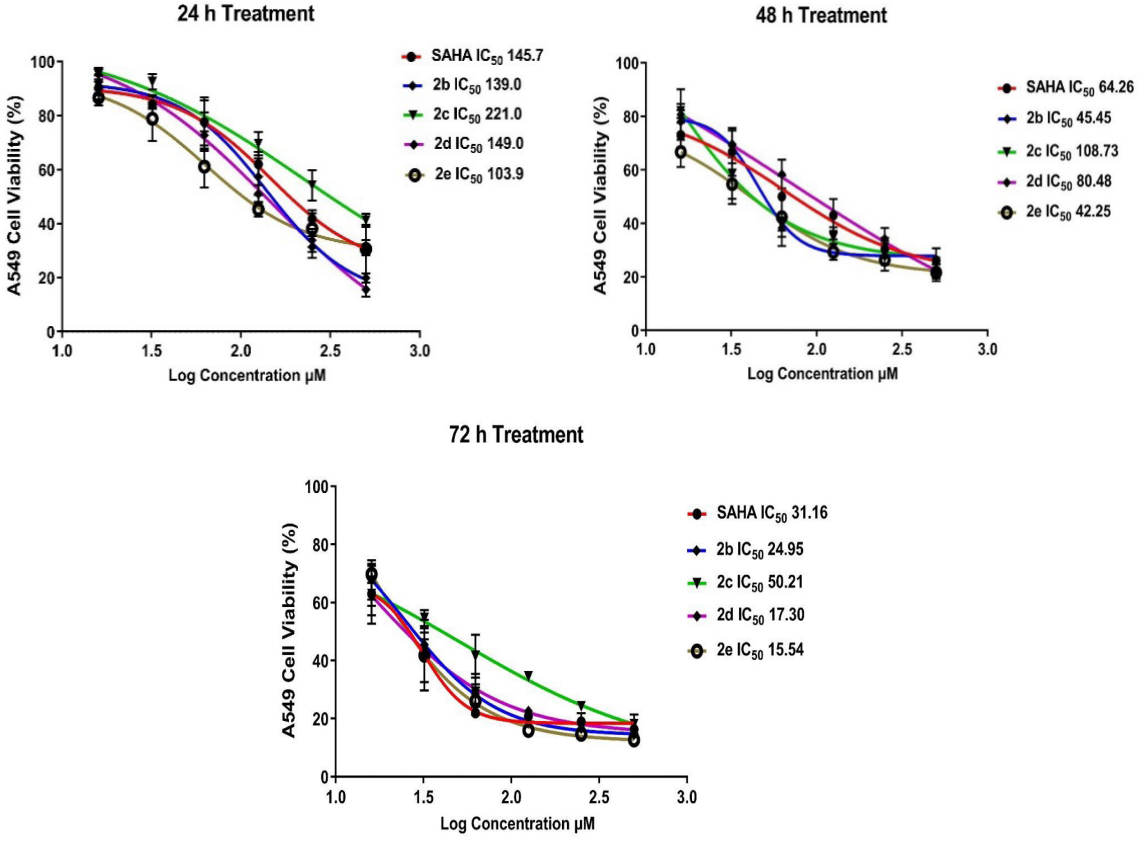

Figure 3. The IC50 values of the investigated compounds against lung cancer cell line (A549) after 24, 48 and 72 hrs treatment and incubation.

structures, as illustrated on Tables 2 and 3. The predicted results have indicated that there was no violation of Lipinski's rule and all the investigated compounds complied with all parameters. However, the results have predicted low passive oral absorption and no penetration into the Blood-Brain Barrier (BBB), as shown on Table 3. This may be due to the violation of other rules such as Veber, Egan, and Muegge. All target compounds have violated these rules because their Total Polar Surface Area (TPSA) is >131.6 for Egan, and >140 for Veber. Additionally, compound 2B has violated Muegge rule because it has a TPSA of >150 (Table 2) [19].

The predicted low oral bioavailability of the target compounds may suggest that the potent compounds could be used through other route of administration. Compounds 2B and 2D may be considered as P-gp substrates. However, compounds 2A, 2C and 2D may exhibit a lower incidence of cellular resistance. SAHA did not show a predictive inhibitory activity to any of the CYP enzymes used in this study. While, compounds 2B, 2D and 2E have shown possible predictive inhibitory activities (Table 3). It is worth mentioning that the cap group and the linker of the presently investigated compounds are considered more versatile due to the presence of more hydrogen bond acceptors and donors. Besides, the optimal length, which is favorable for the interaction with the target enzyme, as indicated by the well-confirmed structure-activity relationships of HDACs inhibitors [20,21].

The interaction of the investigated compounds and SAHA with HDAC8 type 1T69 were comparable to a large extent showing that these target compounds bound to the target enzyme on approximately the same amino acids (Table 1). This may indicate that these compounds may have certain inhibitory activity resembling that of SAHA. However, compound 2E has recorded a remarkable result of binding affinity (docking score) of –9.460, and hence, is expected to have a much higher activity than SAHA. Moreover, this hybrid molecule has interacted to the target enzyme in a much similar way in comparison with SAHA (Figure 1). SAHA has interacted on Asp101, His142, Tyr306, and Zinc378 of the target enzyme. While, compound 2E has interacted with His142, Tyr306, Zinc 378 with a very high docking score than SAHA.

Cytotoxicity *in vitro* evaluation

The determination of the half-maximal inhibitory concentration (IC50) of the hybrid molecules has revealed that compounds 2B, 2D and 2E have showed significant and remarkable activity on lung cancer cell line type A549, potent than SAHA results, particularly after 72 hrs incubation time (Table 4).

Moreover, dose-response curves were constructed to evaluate the relationship between the percent inhibitions of the cell line activity of A549 by the synthesized compounds in comparison with SAHA (Figure 3). The results revealed that there is a great similarity in the pattern of the relationship. This is an expected result due to the great similarity in chemical structures of this series of compounds and SAHA.

Discussion

The highest predicted activity of compound 2E may be due to the rigidity of the aromatic ring which enforces the molecule to take a specific pose directed toward Zinc ions, forming a stronger interaction, as shown in Figure 1. Moreover, this compound may form a π- π interaction (π-π stacking) with the aromatic amino acid residues (such as L-Tyrosine, L-Phenylalanine and L-Histidine) lining the hydrophobic tunnel of the active site near the Zinc ions, as previously reported [22]. The significance of the aromatic linker has been evident in developing several HDACs inhibitors, such as, tubastatin A, belinostat and quisinostat [23].

The predicted results of low passive oral absorption and no penetration into the Blood-Brain Barrier (BBB) may be due to the violation of other rules such as Veber, Egan and Muegge. All the target compounds (2A-E) have violated these rules because their Total Polar Surface Area (TPSA) is >131.6 for Egan, and >140 for Veber. Moreover, compound 2B has violated Muegge rule because of the high TPSA of >150 (Table 2). Results have indicated that SAHA did not show a predictive inhibitory activity to any of the CYP enzymes, while, compounds 2B, 2D and 2E have shown possible predictive inhibitory activities. This may be due to the presence of versatile groups, such as, SH of L-Cysteine, (-CH_2 -)4 and p-aminobenzoic acid, which represent the linker in the side chain, and add more hydrogen bond acceptors and donors, beside the long chain of four –CH_2-, which provide hydrophobicity that is favorable for perfect binding or interaction with target enzyme. A similar case was noticed with the FDA-Approved drug, Panobinostat as powerful HDAC inhibitor [24]. This situation is highly indicated by the well-confirmed structure-activity relationships of HDACs inhibitors. It was reported that the presence of 6-aminohexanoic hydroxamate, prominently induced the differentiation of mouse neuroblastoma cells at sub-millimolar concentrations. This is a similar case with compound 2D, which include benzothiazole-linked to aminohexanoic hydroxamate and afforded significant activity on lung cancer cell line A549 (Table 4).

Previously, new benzothiazole analogues containing aliphatic side chain and based on SAHA exhibited potent HDAC inhibition and cytotoxicity against five cancer cell lines, namely colon cancer SW620, breast cancer MCF-7, prostate cancer PC-3, pancreatic cancer AsPC-1 and lung cancer NCI-H460.

Conclusion

New hybrid molecules of Benzothiazole cross-linked with hydroxamic acid through an amino acid or aminoalkanoic acid linkers were successfully prepared and their binding affinities to HDAC8 (PDB ID: 1T69) were higher than the reference ligand, SAHA. Moreover, the aromatic linker in compound 2E has recorded the highest docking score than SAHA and the other hybrid molecules. Compounds 2A, 2C and 2D are not shown to be P-gp substrates. Therefore, this work may introduce new hybrid molecules (compounds 2B, 2D and 2E) with significant anticancer activity when compared with the reference drug SAHA. Moreover, compound 2E is a promising and potential successful candidate.

Consent for Publication

All authors agree with the content of the article and are listed as co-authors.

Funding Details

This project was financed and supported by college of pharmacy, University of Al-Mustanseryia and Department of Pharmacy, Al-Farabi University College, Baghdad.

Declaration of Competing Interest

The authors declare that they have no known competing financial interests or personal relationships that could have appeared to influence the work reported in this article.

Credit Authorship Contribution Statement

Conceptualization and all the investigations, methodology and draft writing were equally performed by all authors working as a team.

Acknowledgement

We gratefully acknowledge Dr. Woorud for performing the cytotoxicity *in vitro* evaluation.

References

1. Sharma, Prabodh Chander, Diksha Sharma, Archana Sharma and Kushal Kumar Bansal, et al. "New horizons in benzothiazole scaffold for cancer therapy: Advances in bioactivity, functionality, and chemistry." *Appl Mater Today* 20 (2020): 100783.
2. Ali, Samer Abbas. "Synthesis and preliminary antibacterial study of new 2-mercapto-1, 3-benzothiazole derivatives with expected biological activity." AJPS13 (1) (2013).
3. Qiu, Xiaoyan, Xiong Xiao, Nan Li and Yuemin Li. "Histone Deacetylases inhibitors (HDACis) as novel therapeutic application in various clinical diseases." *Prog Neuropsychopharmacol Biol Psychiatry* 72 (2017): 60-72.
4. Shah, Rashmi R. "Safety and tolerability of Histone Deacetylase (HDAC) inhibitors in oncology." *Drug Saf* 42 (2019): 235-245.
5. Eckschlager, Tomas, Johana Plch, Marie Stiborova and Jan Hrabeta. "Histone deacetylase inhibitors as anticancer drugs." *Int J Mol Sci* 18 (2017): 1414.
6. Duvic, Madeleine and Jenny Vu. "Vorinostat: A new oral histone deacetylase inhibitor approved for cutaneous T-cell lymphoma." *Expert Opin Investig Drugs* 16 (2007): 1111-1120.
7. Li, Guo, Yuan Tian and Wei-Guo Zhu. "The roles of histone deacetylases and their inhibitors in cancer therapy." *Front Cell Dev Biol* 8 (2020): 576946.
8. Deng, Bin, Qing Luo, Alexander Halim and Qiuping Liu, et al. "The antiangiogenesis role of histone deacetylase inhibitors: Their potential application to tumor therapy and tissue repair." *DNA Cell Biol* 39 (2020): 167-176.
9. Mishra, Sahil and Palwinder Singh. "Hybrid molecules: The privileged scaffolds for various pharmaceuticals." *Eur J Med Chem* 124 (2016): 500-536.
10. Szumilak, Marta, Anna Wiktorowska-Owczarek and Andrzej Stanczak. "Hybrid drugs-a strategy for overcoming anticancer drug resistance?." *Mol* 26 (2021): 2601.
11. Feng, Lian-Shun, Zhi Xu, Le Chang and Chuan Li, et al. "Hybrid molecules with potential *in vitro* antiplasmodial and *in vivo* antimalarial activity against drug-resistant Plasmodium falciparum." *Med Res Rev* 40 (2020): 931-971.
12. Kerru, Nagaraju, Parvesh Singh, Neil Koorbanally and Raghu Raj, et al. "Recent advances (2015-2016) in anticancer hybrids." *Eur J Med Chem* 142 (2017): 179-212.
13. Thanh Tung, Truong, Dao Thi Kim Oanh, Phan Thi Phuong Dung and Thi My Van Hue, et al. "New benzothiazole/thiazole-containing hydroxamic acids as potent histone deacetylase inhibitors and antitumor agents." *Med Chem* 9 (2013): 1051-1057.
14. Hu, Liu, Xing Cai, Suzhen Dong and Yongjia Zhen, et al. "Synthesis and anticancer activity of novel actinonin derivatives as HsPDF inhibitors." *J Med Chem* 63 (2020): 6959-6978.
15. Noguchi, Takuya, Masahiro Sekine, Yuki Yokoo and Seunghee Jung, et al. "Convenient preparation of primary amides *via* activation of carboxylic acids with ethyl chloroformate and triethylamine under mild conditions." *Chem Lett* 42 (2013): 580-582.
16. Chang, Jin, Hongyu Ren, Mingxia Zhao and Yan Chong, et al. "Development of a series of novel 4-anlinoquinazoline derivatives possessing quinazoline skeleton: Design, synthesis, EGFR kinase inhibitory efficacy, and evaluation of anticancer activities *in vitro*." *Eur J Med Chem* 138 (2017): 669-688.
17. Lipinski, Christopher A., Franco Lombardo, Beryl W. Dominy and Paul J. Feeney. "Experimental and computational approaches to estimate solubility and permeability in drug discovery and development settings." *Adv Drug Deliv Rev* 64 (2012): 4-17.
18. Sandrone, Giovanni, Cyprian D. Cukier, Karol Zrubek and Mattia Marchini, et al. "Role of fluorination in the Histone Deacetylase 6 (HDAC6) selectivity of benzohydroxamate-based inhibitors." *ACS Med Chem Lett* 12 (2021): 1810-1817.
19. Reßing, Nina, Julian Schliehe-Diecks, Paris R. Watson and Melf So ¨nnichsen, et al. "Development of fluorinated peptoid-based Histone Deacetylase (HDAC) inhibitors for therapy-resistant acute leukemia." *J Med Chem* 65 (2022): 15457-15472.
20. Rajak, H., A. Singh, K. Raghuwanshi and R. Kumar, et al. "A structural insight into hydroxamic acid based histone deacetylase inhibitors for the presence of anticancer activity." *Curr Med Chem* 21 (2014): 2642-2664.
21. Bailey, Hanna, David D. Stenehjem and Sunil Sharma. "Panobinostat for the treatment of multiple myeloma: The evidence to date." *J Blood Med* (2015): 269-276.
22. Kraft, Fabian B., Maria Hanl, Felix Feller and Linda Schäker-Hübner, et al. "Photocaged histone deacetylase inhibitors as prodrugs in targeted cancer therapy." *Pharm* 16 (2023): 356.
23. Lu, Jiebo, Zong Ping Chen, Yong Ping Yan and Spencer Knapp, et al. "Aminohexanoic hydroxamate is a potent inducer of the differentiation of mouse neuroblastoma cells." *Cancer Lett* 160 (2000): 59-66.
24. Oanh, Dao Thi Kim, Hoang Van Hai, Sang Ho Park and Hyun-Jung Kim, et al. "Benzothiazole-containing hydroxamic acids as histone deacetylase inhibitors and antitumor agents." *Bioorganic Med Chem Lett* 21 (2011): 7509-7512.

How to cite this article: Abdul-Hameed, Yazen, Shakir M. Alwan and Ashour H. Dawood. "Molecular Docking, Synthesis and Preliminary Evaluation of Hybrid Molecules of Benzothiazole Cross-linked with Hydroxamic Acid by Certain Linkers as HDAC Inhibitors." *Med Chem* 13 (2023): 687.